Applied Physics Letters

B-site disorder driven multiple-magnetic phases: Griffiths phase, re-entrant cluster glass, and exchange bias in Pr_2CoFeO_6

Cite as: Appl. Phys. Lett. **114**, 252403 (2019); https://doi.org/10.1063/1.5094905
Submitted: 06 March 2019 . Accepted: 12 June 2019 . Published Online: 26 June 2019

Arkadeb Pal, Prajyoti Singh, V. K. Gangwar, Surajit Ghosh, P. Prakash, S. K. Saha, Amitabh Das, Manoranjan Kumar, A. K. Ghosh, and Sandip Chatterjee

Applied Physics Letters ARTICLE scitation.org/journal/apl

B-site disorder driven multiple-magnetic phases: Griffiths phase, re-entrant cluster glass, and exchange bias in Pr_2CoFeO_6

Cite as: Appl. Phys. Lett. **114**, 252403 (2019); doi: 10.1063/1.5094905
Submitted: 6 March 2019 · Accepted: 12 June 2019 ·
Published Online: 26 June 2019

View Online Export Citation CrossMark

Arkadeb Pal,[1] Prajyoti Singh,[1] V. K. Gangwar,[1] Surajit Ghosh,[1] P. Prakash,[2] S. K. Saha,[3] Amitabh Das,[2,4] Manoranjan Kumar,[3] A. K. Ghosh,[5] and Sandip Chatterjee[1,a)]

AFFILIATIONS

[1]Indian Institute of Technology (BHU), Varanasi 221005, India
[2]Solid State Physics Division, Bhabha Atomic Research Centre, Mumbai 400085, India
[3]S. N. Bose National Centre for Basic Sciences, Kolkata 700098, India
[4]Homi Bhabha National Institute, Anushaktinagar, Mumbai 400094, India
[5]Banaras Hindu University, Varanasi 221005, India

[a)]Author to whom correspondence should be addressed: schatterji.app@iitbhu.ac.in

ABSTRACT

The magnetic spin ordering and the magnetization dynamics of a double perovskite Pr_2CoFeO_6 have been investigated by employing the (dc and ac) magnetization and neutron powder diffraction techniques. The study revealed that Pr_2CoFeO_6 adopted a B-site disordered orthorhombic structure (Pnma). Furthermore, *ab initio* band structure calculations suggested an insulating antiferromagnetic ground state. Magnetization measurements revealed that the system possesses a spectrum of competing magnetic phases, viz., long range canted antiferromagnetic (AFM) spin ordering ($T_N \sim 269$ K), Griffiths-like phase, re-entrant cluster glass ($T_G \sim 34$ K), and exchange bias effects. The neutron diffraction study divulged the exhibition of a long range G-type of canted AFM spin ordering. The random nonmagnetic dilution of magnetic Fe^{3+} (high spin) ions by Co^{3+} (low spin) ions due to B-site disorder essentially played a crucial role in manifesting such magnetic properties of the system.

The class of double perovskites (DPs) $A_2BB'O_6$ has attracted a great deal of research attention owing to their diverse exotic properties, viz., giant magnetoresistance, magnetocaloric effects, antisite disorder driven multiglass phases, giant exchange bias (EB), Griffiths phase (GP), etc., which can be harnessed to fabricate innovative devices for practical applications.[1–6] Moreover, observation of multiple properties in a single material is highly interesting as next generation spintronic devices are progressively predicated upon discovering new multifunctional materials.

In the present letter, we have reported the coexistence of GP, the re-entrant glassy state, and the exchange bias (EB) effect in antiferromagnetic Pr_2CoFeO_6 (PCFO). In fact, a ferromagnetic (FM) system was initially thought to be a prerequisite for exhibition of GP.[4,7–11] However, recently, GP has been reported in a very few antiferromagnetic (AFM) systems, but the observation of the same around room temperature is very scarce.[12–15] On the other hand, glassy states emanate from the spin frustrations.[16–24] Apart from its intriguing rich physics, it helped envisaging many real world practical applications.[25,26] Eventually, as compared to the large number of systems exhibiting spin-glass (SG) states, fewer systems are reported to show re-entrant SG states.[5,23,24] Furthermore, in contrast to the widely studied ordered $A_2BB'O_6$ (B/B′ = Mn, Co, Ni) DPs, the studies on the Fe based site-disordered DPs, i.e., R_2BFeO_6 oxides, are comparatively limited, and thus, there are much more opportunities to explore their properties.[6,27–30] Recently, the detailed electronic structure study of PCFO revealed the trivalent oxidation states for Co and Fe ions.[28]

The polycrystalline Pr_2CoFeO_6 sample was prepared by the conventional solid state reaction method.[28] The neutron diffraction measurements (using unpolarized neutrons) were carried out on a PD2 neutron powder diffractometer ($\lambda = 1.2443$ Å) at the Dhruva reactor in the Bhabha Atomic Research Centre, Mumbai, India. A SQUID based magnetic property measurement system (Quantum Design) was employed for magnetization measurements of a small pellet of the sample.

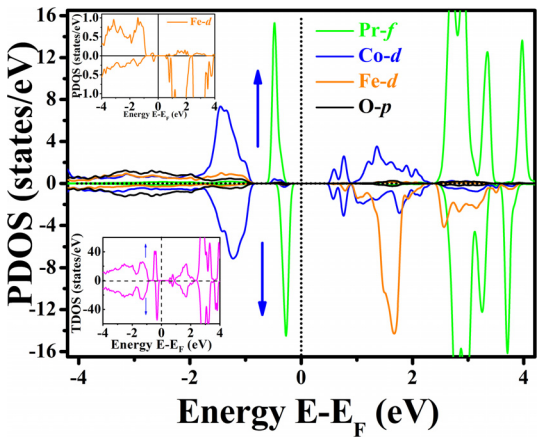

FIG. 1. Spin resolved PDOS for Pr-*f*, Co-*d*, Fe-*d*, and O-*p* orbitals. Its top and bottom insets show the PDOS (enlarged) of Fe-3d and TDOS of PCFO, respectively.

In the theoretical study, we have performed the *ab initio* calculations based on density function theory (DFT) using Vienna *ab initio* simulation package (VASP).[47] Exchange-correlation potential (Perdew-Burke-Ernzerhof exchange-correlation functional) is approximated with generalized gradient approximation (GGA).[31] The projector augmented wave method (PAW) is used for core-valence interaction.[32] The calculations were performed with a K-mesh of $8 \times 5 \times 8$ with the Pnma space group. To calculate the spin polarized partial and total density of states (DOS), we have considered the on-site coulomb correction (GGA+U). The Hubbard U corrections are considered to be ~3 eV for Pr-4f states,[33] ~3 eV for Co-3d states,[34] and ~4 eV for Fe-3d states.[35] The calculation predicted an AFM ground state of PCFO as the AFM couplings among spins were found to be energetically favorable than FM couplings. The total density of states (TDOS) of PCFO for the AFM interactions is shown in the inset (bottom) of Fig. 1. The absence of any states near the Fermi level suggests an insulating nature of the system. Moreover, it was observed that Pr-*f*, Co-*d*, Fe-*d*, and O-*p* states have the dominant contribution in their respective spin integrated partial density of states (PDOS) (supplementary material). Figure 1 depicts the spin resolved PDOS for Pr-*f*, Co-*d*, Fe-*d*, and O-*p* states. It is clear from the PDOS curves that there is significant hybridization among Co/Fe-*3d* and O-*2p* states. The large asymmetry observed in Fe-*3d* PDOS clearly suggests its magnetic nature (top inset of Fig. 1). The corresponding magnetic moment of Fe is found to be ~4.43 μ_B. However, Co-*3d* and O-*2p* PDOSs do not show any significant spin polarization (asymmetry), thus suggesting the nonmagnetic nature of these ions. The nonmagnetic low spin (LS) nature of Co^{3+} corroborates with our earlier work on PCFO as well as other reports on similar systems, viz., $RCoO_3$, Ho_2CoFeO_6, La_2CoFeO_6, etc.[6,27,28,33,34]

We have performed the neutron powder diffraction (NPD) study to get an insight into its microscopic spin structure and B-site structural ordering [the large difference in the coherent neutron scattering lengths of Co (2.49 fm) and Fe (9.45 fm) makes it possible to probe it]. The neutron thermodiffractograms along with its Rietveld refinements at 300 K (Pnma) and 6 K (Pnma+ magnetic phase P-1) are shown in Figs. 2(a) and 2(b). The refinements suggest that the compound crystallizes in the B-site disordered (Co/Fe shares the same site 4b) orthorhombic structure. The detailed summary of the obtained structural parameters can be found in Table 1 of the supplementary material. The reduced bond angle of Co(Fe)-O1-Co(Fe) is found to be 159.03° (at 300 K), which indicates the presence of octahedral distortion due to the smaller size or Pr^{3+} ions. Apart from this, the calculated bond lengths of Fe/Co-O showed a close match with the theoretical bond length for high spin Fe^{3+} (HS) and low spin Co^{3+} (LS) ions (supplementary material).

Interestingly, NPD data recorded at 6 K show an intense superlattice reflection peak (011) at ~16° which was absent at 300 K. The

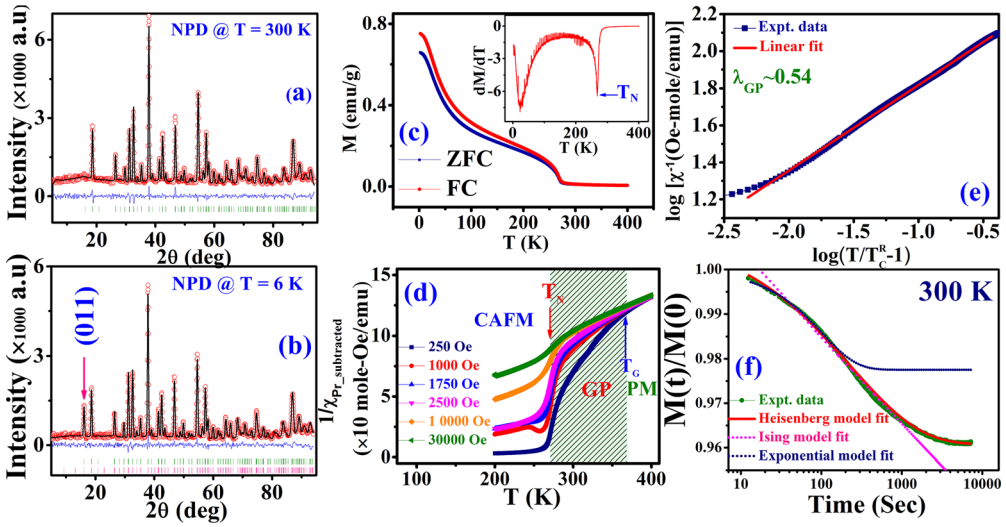

FIG. 2. (a) and (b) depict the NPD pattern at 300 K and 6 K, respectively. (c) ZFC-FC M(T) curves for H = 250 Oe, while its inset shows the "dM/dT vs T" curve. (d) demonstrates the χ_{Pr} subtracted "χ^{-1} vs T" plot at different fields. (e) depicts the power law fit for GP. (f) shows the TRM data at 300 K along with their Heisenberg, Ising, and exponential fits.

nuclear contribution to this reflection (011) is absent or minimal, while it has significant contribution from magnetic phase P-1. Moreover, the refined NPD pattern analysis yielded a G_zF_y type of canted AFM spin structure for PCFO where the FM and the G-type AFM moments occur along y and z-directions, respectively, (supplementary material).[27] The analysis of NPD data at 6 K gives the moment values of 1.8 μ_B and 0.6 μ_B for the AFM and FM contributions, respectively, (per Fe ion), thus suggesting predominant AFM interactions in the system. Both the AFM and FM moments exhibited a drastic jump below 275 K, indicating a magnetic phase transition below this temperature (supplementary material). Eventually, below 275 K, the refined site moments are found to be in the range of 1.5–2 μ_B (per Fe ion), which are comparable to the theoretically expected average moment of ~2.5 μ_B for Co^{3+} (LS, S = 0) and Fe^{3+} (HS, S = 5/2) ions. In contrast, for Co^{3+} (HS, S = 2) and Fe^{3+} (HS, S = 5/2) ions, the theoretically predicted moment value is 4.5 μ_B which is a much higher value than the experimental values. Hence, the analysis also suggests the low spin state (LS) for Co^{3+}.

Furthermore, in the dc "magnetization (M) vs temperature (T)" study with zero field cooled (ZFC) and field cooled (FC) protocols, a sharp jump in M can be observed below $T_N \sim 269$ K, which suggests for a magnetic transition and agrees well with the NPD data [Fig. 2(c)]. The observed thermomagnetic irreversibility between FC and ZFC arms suggests the existence of competing spin interactions or spin frustrations. The exact transition temperature T_N was identified from the inflection point of the temperature dependent (dM/dT) curve at ~269 K [inset Fig. 2(c)]. The same was determined from the ac susceptibility measurements which showed sharp and frequency independent χ' peaks at ~269 K, thus confirming the onset of long range ordering (supplementary material). The Curie-Weiss (CW) fit of the susceptibility data also suggested the existence of HS Fe^{3+} and LS Co^{3+} ions in PCFO (supplementary material). The isothermal field variation of magnetization (M-H) curves near T_N showed small hysteresis but nonsaturating behavior even at a high field of 40 kOe, thus indicating predominant AFM nature (supplementary material). The FM hysteretic feature arises due to the canting of Fe^{3+} spins by the Dzyaloshinskii-Moriya interactions which are commonly observed in orthoferrites.[6,27,36,37]

To exclude paramagnetic (PM) Pr^{3+} spin contribution, we have subtracted the susceptibility of a standard system of $PrAlO_3$ from that of PCFO (supplementary material). Thus, we have obtained the susceptibility which is mainly due to the B-site ions of PCFO. Most interestingly, "temperature variation of inverse susceptibility χ^{-1} (Pr-subtracted)" curves [Fig. 2(d)] at different applied fields showed a rapid down-turn deviation from CW behavior at temperatures well-above T_N. This feature is a hallmark for a special magnetic phase known as the Griffiths phase (GP) where the system neither behaves like a paramagnet nor shows long range ordering.[9–15] In fact, the observation of down-turn behavior of χ^{-1} (T) at low fields is very crucial as it eventually helps one to distinguish the Griffiths phase from other non-Griffiths-like clustered phases, where χ^{-1} (T) deviates from the CW law by showing an up-turn above ordering temperature.[10] From Fig. 2(d), it is also clear that the down-turn deviation gets softened with increasing magnetic fields, and with sufficiently high magnetic fields, it yields CW-like behavior which is also a hallmark for the Griffiths phase.[10] It is because of the fact that the magnetization increases linearly with magnetic fields in paramagnetic regions, and thus, at high fields, PM susceptibility dominates over the contribution from the correlated clusters to the susceptibility. The GP evolves due to the nucleation of finite sized correlated regions or/and clusters having short range magnetic ordering embedded in the global paramagnetic matrix above magnetic transition temperature. In the GP regime, magnetization follows a power law with a characteristic nonuniversal exponent λ,[9]

$$\chi^{-1}(T) \propto (T - T_c^R)^{1-\lambda} \quad (0 < \lambda < 1). \tag{1}$$

Here, the parameter λ is a measure of deviation from CW behavior and T_c^R is the magnetic transition temperature of the random non-magnetic ion diluted system.[7,8] The GP temperature is estimated to be $T_G \sim 370$ K below which the down-turn behavior commences violating the CW law. To confirm GP and estimate the value of λ, we have followed the same approach as used by Karmakar *et al.* by taking $T_c^R = T_N$.[13] Figure 2(e) depicts the $\log_{10}$-$\log_{10}$ plot of "χ^{-1} vs $(T/T_c^R - 1)$" for 250 Oe data, where the linear fitting in the GP region yielded $\lambda \sim 0.54$ which confirms the Griffiths phase.

However, knowing that the spin dynamics in GP behaves different from that in the PM phase, we have used the following two models for interacting spins in the GP regime described by the spin autocorrelation function C(t) as follows:[38]

$$C(t) \propto exp(-A(lnt^{\frac{d}{d-1}})) : \text{For Ising system,} \tag{2}$$

$$C(t) \propto exp(-Bt^{\frac{1}{2}}) : \text{For Heisenberg System.} \tag{3}$$

For this, we have carried out isothermal temporal remanent magnetization (TRM) measurements to further confirm GP. A field cooling of the sample with H = 10 kOe is done from 400 K to the desired temperatures in GP. The "residual magnetization as a function of time" at 300 K and 325 K was recorded after sudden removal of the field. Interestingly, both the TRM data showed the best fit with the Heisenberg spin model, while it deviated from exponential as well as Ising model decay schemes [Fig. 2(f) shows fits of data taken at 300 K, while those at 325 K are shown in the supplementary material]. Therefore, it indicates that the system is not in the simple paramagnetic state above T_N, rather there exists GP which eventually slows down the spin dynamics.

In the pioneering work by Imry and Ma, the random quenched disorder was reported to hinder the formation of long range ordering, thereby favoring the nucleation of correlated clusters.[39] Thereafter, quenched disorder has remained a key factor for producing GP in many systems.[9–11,40–43] Therefore, the observed GP in PCFO may be attributed to the quenched disorder associated with the random distribution of the ions Co^{3+} (LS) and Fe^{3+} at site 4b.[8–11,40–43] Additionally, the spin canting introduces the competitive AFM/FM interactions which together with the B-site disorder create random exchange interactions (not only by its values but also by its signs), and this can also be a plausible origin of the observed GP. Further, the observed octahedral distortion in PCFO causing the concurrent changes in the Fe^{3+}-O-Fe^{3+} exchange interactions may also play an important role in the evolution of GP.[9]

Apart from this, we reiterate that the magnetization curves showed a sudden slope change at lower temperatures; hence, to probe if there exist any secondary magnetic phases, we have further performed ac susceptibility measurements. The curves $\chi'(T)$ show distinct anomaly below 40 K, and the corresponding broad

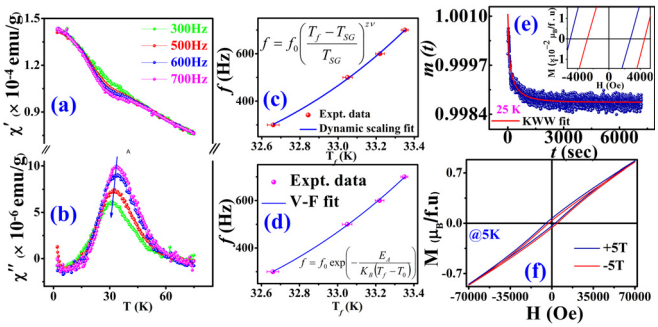

FIG. 3. (a) and (b) depict ac $\chi'(T)$ and $\chi''(T)$ curves, respectively. (c) and (d) show dynamic scaling and Vogel-Fulcher fits of the "T_f vs f" curve, respectively. (e) TRM at 25 K along with the KWW fit. (f) M(H) curves at 5 K with cooling fields ±5 T. The inset of (e) depicts the enlarged view of these M(H) curves at 5 K.

and frequency dependent $\chi''(T)$ (Kramers–Kronig) peaks are clearly observed near ∼34 K, which is a typical feature of the spin glass (SG) state [Figs. 3(a) and 3(b)].[16–24] Hence, it is comprehensible that it enters in a re-entrant spin-glass (RSG)-like state at lower temperatures. The frequency sensitivity of T_f has been estimated by the Mydosh parameter (p) which is a universal tool to distinguish glassy states[44]

$$p = \frac{\Delta T_f}{T_f \Delta log_{10}(f)}. \tag{4}$$

For typical SG, $p < 0.01$ and for super paramagnetic (SP) system, $p > 0.1$, while for cluster glass (CG), it has intermediate values between SG and SP. The obtained value of $p \sim 0.05$ lies in the realm of CG systems.

Eventually, the spin dynamics in a glassy state gets slowed down below the critical temperatures T_f which can be investigated using the dynamic scaling law[17,22]

$$f = f_0 \left(\frac{T_f - T_{SG}}{T_{SG}}\right)^{z\nu}, \tag{5}$$

where f refers to the frequency for $\chi''(T)$ curves attaining a maximum at $T = T_f$, T_{SG} is the equivalent SG freezing temperature with $f \to 0$ Hz and $H_{DC} \to 0$ Oe, and f_0 is related to the characteristic spin flipping time (τ_0 as $f_0 = \frac{1}{\tau_0}$); $z\nu$ is the dynamical critical exponent. The best fitting of the "f vs T_f" curve yielded $f_0 \sim 10^6$ Hz ($\tau_0 \sim 10^{-7}$ s), $T_{SG} = 29.21 \pm 08$ K, and $z\nu \sim 4.6 \pm 0.2$ (which is satisfactory for SG/CG: $4 < z\nu < 12$) [Fig. 3(c)]. For a canonical SG system, τ_0 lies between $\sim 10^{-12}$ and 10^{-13} s which is smaller than the observed value of $\sim 10^{-7}$ s by few orders. The larger τ_0 indicates toward freezing of magnetic clusters rather than atomic spins.[17,22] To further investigate intercluster interactions, the empirical Vogel-Fulcher (VF) model [described by Eq. (6)] was employed in fitting the "f vs T_f" curve [Fig. 3(d)]

$$f = f_0 exp\left(\frac{-E_A}{K_B(T_f - T_0)}\right), \tag{6}$$

where T_0 represents intercluster interaction strength and E_A is the activation energy. The best fitting yielded $f_0 \sim 10^6$ Hz, $T_0 = 27.45 \pm 0.17$ K, and $E_A/K_B = 37.4 \pm 1.4$ K. The comparable values of T_0 and E_A indicate the existence of strong intercluster couplings in the system. Again, the larger value of τ_0 suggests for the re-entrant cluster glass (RCG) state.

Moreover, isothermal temporal relaxation of the remanent magnetization (TRM) at 25 K was performed to further confirm the glassy state with a cooling field of H = 0.1 T [Fig. 3(e)]. TRM data were analyzed using the KWW (Kohlrausch Williams Watt) stretched exponential equation[18]

$$m(t) = m_0 - m_g exp\left\{-\left(\frac{t}{\tau}\right)^{\beta}\right\}. \tag{7}$$

Here, m_0 is the initial remanent magnetization, m_g is the magnetization of the glassy component, τ is the characteristic relaxation time constant, and β is the stretching exponent. The KWW method is widely used for the investigations of glassy systems for which β lies in between 0 and 1. Thus, the obtained β value $\sim 0.52 \pm 0.02$ from the best fit further confirms the existence of the CG state. Eventually, the coexistence of long range ordering with the lower temperature re-entrant spin-cluster glass phase is very interesting and has been reported in different systems, viz., AFM $PbFe_{0.5}Nb_{0.5}O_3$, $BiMnFe_2O_6$, $LiMn_2O_4$, etc.[45,46]

The present system essentially contains the two major microscopic ingredients for glassy transitions: (i) B-site disorder and (ii) Spin canting.[5,19,23] In pure FM or AFM systems, the domain formation involves microscopic time scales, but due to the presence of site-disorder, it causes pinning of the domain wall, which essentially gives rise to metastable states. It does not allow the system to attain an equilibrium state in the experimental time scale, leading to nonequilibrium phases such as spin-relaxations and aging effects.[19,24] In PCFO, the B-site disorder causes the local environment of the magnetic spins to be inhomogeneous. The concomitant spin frustration emanating random exchange interactions at low temperatures ends up in random, noncollinear, frozen states of spins, leading to the RCG state. Again, the presence of spin canting in PCFO is also an important and potential ingredient for the glassy state, which can essentially cause random, partial spin freezing, thus leading to the RSG or RCG states.[20,23]

Moreover, the coexistence of long range ordering with lower temperature glassy states often leads to the exchange bias (EB) effect.[46] Hence, to further explore the coexistence of AFM and CG states in PCFO, we have carried out the EB effect experiment. The sample was cooled in a magnetic field of ±5 T down to 5 K, and M-H loops were recorded [Fig. 3(f)]. The EB effect is evidenced from the clear horizontal shift of the M(H) loop along the negative (positive) field axis with the positive (negative) cooling field [inset Fig. 3(e)].[46–48] We have obtained an appreciable value of the EB field: $H_{EB} \sim 2175$ Oe, where $H_{EB} = \frac{|H_{c1} - H_{c2}|}{2}$ and H_{C1} and H_{C2} are the negative or positive intercepts along the field axis with +5 T and −5 T, respectively. The observed EB effect can be elucidated by the coexistence of AFM clusters in the frozen glassy spin matrix.[46] Due to the strong nonswitchable unidirectional pinning forces or exchange anisotropy induced at the interfaces of the AFM spin-clusters/glassy spin matrix, the M(H) loop gets shifted exhibiting the EB effect.[46]

In summary, the crucial roles of B-site disorder have been thoroughly brought out in the evolution of a spectrum of interesting magnetic properties like GP, RCG, and EB effects in Pr_2CoFeO_6. The

observation of maidenly recognized GP in the AFM PCFO system essentially places it among the rare materials which order antiferromagnetically and exhibit GP.

See the supplementary material for some additional information related to DFT, NPD, and magnetization studies as mentioned in the main text.

The authors are grateful to the Central Instrumentation Facility Centre, Indian Institute of Technology (BHU), for providing the MPMS facility.

REFERENCES

[1]K. I. Kobayashi, T. Kimura, H. Sawada, K. Terakura, and Y. Tokura, Nature **395**, 677 (1998).
[2]R. I. Dass and J. B. Goodenough, Phys. Rev. B **67**, 014401 (2003).
[3]N. S. Rogado, J. Li, A. W. Sleight, and M. A. Subramanian, Adv. Mater. **17**, 2225 (2005).
[4]H. S. Nair, D. Swain, N. Hariharan, S. Adiga, C. Narayana, and S. Elizabeth, J. Appl. Phys. **110**, 123919 (2011).
[5]D. Choudhury, P. Mandal, R. Mathieu, A. Hazarika, S. Rajan, A. Sundaresan, U. V. Waghmare, R. Knut, O. Karis, P. Nordblad *et al.*, Phys. Rev. Lett. **108**, 127201 (2012).
[6]G. R. Haripriya, H. S. Nair, R. Pradheesh, S. Rayaprol, V. Siruguri, D. Singh, R. Venkatesh, V. Ganesan, K. Sethupathi, and V. Sankaranarayanan, J. Phys.: Condens. Matter **29**, 475804 (2017).
[7]R. B. Griffiths, Phys. Rev. Lett. **23**, 17 (1969).
[8]A. J. Bray and M. A. Moore, J. Phys. C **15**, L765 (1982).
[9]M. B. Salamon, P. Lin, and S. H. Chun, Phys. Rev. Lett. **88**, 197203 (2002).
[10]C. He, M. A. Torija, J. Wu, J. W. Lynn, H. Zheng, J. F. Mitchell, and C. Leighton, Phys. Rev. B **76**, 014401 (2007).
[11]A. K. Pramanik and A. Banerjee, Phys. Rev. B **81**, 024431 (2010).
[12]Z. W. Ouyang, N. M. Xia, Y. Y. Wu, S. S. Sheng, J. Chen, Z. C. Xia, L. Li, and G. H. Rao, Phys. Rev. B **84**, 054435 (2011).
[13]A. Karmakar, S. Majumdar, S. Kundu, T. K. Nath, and S. Giri, J. Phys.: Condens. Matter **25**, 066006 (2013).
[14]K. Ghosh, C. Mazumdar, R. Ranganathan, and S. Mukherjee, Sci. Rep. **5**, 15801 (2015).
[15]J. Kumar, S. N. Panja, S. Dengre, and S. Nair, Phys. Rev. B **95**, 054401 (2017).
[16]J. A. Mydosh, *Spin Glasses: An Experimental Introduction* (Taylor and Francis, London, 1933).
[17]C. Djurberg, P. Svedlindh, P. Nordblad, M. F. Hansen, F. Bødker, and S. Mørup, Phys. Rev. Lett. **79**, 5154 (1997).
[18]A. Ito, H. Aruga, E. Torikai, M. Kikuchi, Y. Syono, and H. Takei, Phys. Rev. Lett. **57**, 483 (1986).
[19]E. Vincent, V. Dupuis, M. Alba, J. Hammann, and J. P. Bouchaud, Europhys. Lett. **50**, 674 (2000).
[20]P. Mahadevan, F. Aryasetiawan, A. Janotti, and T. Sasaki, Phys. Rev. B **80**, 035106 (2009).
[21]S. Niidera, S. Abiko, and F. Matsubara, Phys. Rev. B **72**, 214402 (2005).
[22]M. D. Mukadam, S. M. Yusuf, P. Sharma, S. K. Kulshreshtha, and G. K. Dey, Phys. Rev. B **72**, 174408 (2005); and references therein.
[23]K. Manna, A. K. Bera, M. Jain, S. Elizabeth, S. M. Yusuf, and P. S. Anil Kumar, Phys. Rev. B **91**, 224420 (2015); and references therein.
[24]L. Shlyk, S. Strobel, B. Farmer, L. E. De Long, and R. Niewa, Phys. Rev. B **97**, 054426 (2018).
[25]L. Personnaz, I. Guyon, and G. Dreyfus, J. Phys. Lett. **46**, 359 (1985); K. Binder and A. P. Young, Rev. Mod. Phys. **58**, 801 (1986).
[26]A. G. Hudetz, C. J. Humphries, and J. R. Binder, Front. Syst. Neurosci. **8**, 234 (2014).
[27]D. V. Karpinsky, I. O. Troyanchuk, K. Barner, H. Szymczak, and M. Tovar, J. Phys.: Condens. Matter **17**, 7219 (2005).
[28]A. Pal, S. Ghosh, A. G. Joshi, S. Kumar, S. Patil, P. K. Gupta, P. Singh, V. K. Gangwar, P. Prakash, R. K. Singh *et al.*, J. Phys.: Condens. Matter **31**, 275802 (2019).
[29]N. Li, F. Fan, F. Sun, Y. Wang, Y. Zhao, F. Liu, Q. Zhang, D. Ikuta, Y. Xiao, P. Chow *et al.*, Phys. Rev. B **99**, 195115 (2019).
[30]K. Yoshimatsu, K. Nogami, K. Watarai, K. Horiba, H. Kumigashira, O. Sakata, T. Oshima, and A. Ohtomo, Phys. Rev. B **91**, 054421 (2015).
[31]J. P. Perdew, K. Burke, and M. Ernzerhof, Phys. Rev. Lett. **77**, 3865 (1996).
[32]P. E. Blochl, Phys. Rev. B **50**, 17953 (1994).
[33]S. K. Pandey, A. Kumar, S. M. Chaudhari, and A. V. Pimpale, J. Phys.: Condens. Matter **18**, 1313 (2006).
[34]S. K. Pandey, A. Kumar, S. Patil, V. R. R. Medicherla, R. S. Singh, K. Maiti, D. Prabhakaran, A. T. Boothroyd, and A. V. Pimpale, Phys. Rev. B **77**, 045123 (2008).
[35]Y. L. Lee, J. Kleis, J. Rossmeisl, and D. Morgan, Phys. Rev. B **80**, 224101 (2009).
[36]I. Dzyaloshinsky, J. Phys. Chem. Solids **4**, 241 (1958); T. Moriya, Phys. Rev. **120**, 91 (1960).
[37]I. Fita, A. Wisniewski, R. Puzniak, E. E. Zubov, V. Markovich, and G. Gorodetsky, Phys. Rev. B **98**, 094421 (2018); and references therein.
[38]A. J. Bray, Phys. Rev. Lett. **60**, 720 (1988).
[39]Y. Imry and S. K. Ma, Phys. Rev. Lett. **35**, 1399 (1975).
[40]J. Deisenhofer, D. Braak, H.-A. K. von Nidda, J. Hemberger, R. M. Eremina, V. A. Ivanshin, A. M. Balbashov, G. Jug, A. Loidl, T. Kimura, and Y. Tokura, Phys. Rev. Lett. **95**, 257202 (2005).
[41]Y. Shimada, S. Miyasaka, R. Kumai, and Y. Tokura, Phys. Rev. B **73**, 134424 (2006).
[42]S. Guo, D. P. Young, R. T. Macaluso, D. A. Browne, N. L. Henderson, J. Y. Chan, L. L. Henry, and J. F. DiTusa, Phys. Rev. Lett. **100**, 017209 (2008).
[43]C. Magen, P. A. Algarabel, L. Morellon, J. P. Araújo, C. Ritter, M. R. Ibarra, A. M. Pereira, and J. B. Sousa, Phys. Rev. Lett. **96**, 167201 (2006).
[44]L. T. Coutrim, E. M. Bittar, F. Stavale, F. Garcia, E. Baggio-Saitovitch, M. Abbate, R. J. O. Mossanek, H. P. Martins, D. Tobia, P. G. Pagliuso *et. al.*, Phys. Rev. B **93**, 174406 (2016); and references therein.
[45]W. Kleemann, V. V. Shvartsman, P. Borisov, and A. Kania, Phys. Rev. Lett. **105**, 257202 (2010).
[46]X. K. Zhang, J. J. Yuan, Y. M. Xie, Y. Yu, F. G. Kuang, H. J. Yu, X. R. Zhu, and H. Shen, Phys. Rev. B **97**, 104405 (2018); and references therein.
[47]W. H. Meiklejohn and C. P. Bean, Phys. Rev. **102**, 1413 (1956).
[48]D. Niebieskikwiat and M. B. Salamon, Phys. Rev. B **72**, 174422 (2005).